

Microbial Diversity in Algerian Hypersaline Environments: Insights from Hadjer El-Melh and Zahrez-Gharbi (Djelfa, Algeria)

Ahmed Beladel^{1*}, Saad Boutaiba², Brahim Beladel³, Fahd Arbaoui⁴, Ahcen Hakem⁵, Aissa Benhamida⁶, Mohammed Mebarek Bia⁷

¹Laboratory of Exploration and Valorization of Steppe Ecosystems (EVES), Department of Biology, Faculty of Natural and Life Sciences, University of Djelfa, Djelfa 17000, Algeria.

* Corresponding Author Email: beladel.ahmed@univ-djelfa.dz - ORCID: 0000-0003-1843-3974

²Laboratory of Exploration and Valorization of Steppe Ecosystems (EVES), Department of Biology, Faculty of Natural and Life Sciences, University of Djelfa, Djelfa 17000, Algeria.

Email: s.boutaiba@univ-djelfa.dz - ORCID: 0000-0003-3893-1786

³Department of Physics, University of Djelfa, Djelfa 17000, Algeria

Email: b.beladel@univ-djelfa.dz - ORCID: 0000-0001-9009-2911

⁴Department of Chemistry, Nuclear Research Center of Birine (CRNB), Algeria

Email: f.arbaoui@crnb.dz - ORCID: 0009-0002-3754-3511

⁵Centre de Recherche en Agropastoralisme – CRAPast

Email: hakem.ahcen@crapast.dz - ORCID: 0009-0002-3755-9038

⁶Université Shahid Hama Lakhdar - El Oued, Algeria

Email: benhamida-aissa@univ-eloued.dz - ORCID: 0009-0002-8945-4182

⁷Department of Parasitology, College of Medicine, Chungbuk National University - Cheongju- South Korea

Email: biamebarek@chungbuk.ac.kr - ORCID: 0000-0003-2495-6800

Article Info:

DOI: 10.22399/ijcesen.5137

Received: 15 November 2025

Revised: 22 January 2026

Accepted: 04 April 2026

Keywords:

Hypersaline environments

Microbial diversity

16S rRNA sequencing

Hadjer El-Melh

Zahrez-Gharbi

Halophiles

Abstract:

Hypersaline environments harbor highly specialized and diverse microbial communities shaped by extreme physicochemical conditions. This study investigates the microbial diversity of two hypersaline water samples from Algeria: Hajr El Meleh (Salt Rock) (S1) and Zahrez-Gharbi (S2). Physicochemical analyses revealed extremely high salinities (26.5% and 23.0% NaCl, respectively), near-neutral pH, and elevated concentrations of Na⁺, Cl⁻, Mg²⁺, and SO₄²⁻. Using 16S rRNA gene amplicon sequencing via the Illumina MiSeq platform, we characterized bacterial and archaeal communities at multiple taxonomic levels. Alpha diversity indices (Chao1, Shannon, ACE) indicated higher species richness and evenness in S1. Taxonomic profiling showed dominance of Firmicutes, Proteobacteria, and Bacteroidota in both sites, with sample-specific phyla such as Halobacterota (S2) and Euryarchaeota (S1). At the family, genus, and species levels, significant variations were observed: S1 was enriched in *Salinibacter*, *Methanobrevibacter smithii*, and *Fingoldia magna*, while S2 was characterized by *Bacillus*, *Veillonella*, and *Campylobacter*. The presence of numerous unclassified taxa across both samples highlights the potential for novel microbial lineages in these extreme habitats. Our findings highlight the patterns of microbial community structure and diversity in relation to salinity, ion composition, and geological context, contributing to the understanding of extremophile adaptation in saline ecosystems.

1. Introduction

Hypersaline environments represent some of the most extreme ecosystems on Earth, characterized by high salt concentrations, strong ionic stress, limited

water activity, and often nutrient scarcity. Despite these harsh conditions, they harbor a wide range of halophilic and halotolerant microorganisms both bacterial and archaeal that have developed unique physiological and molecular adaptations for survival

(Oren, 2010; Ventosa et al., 2015; DasSarma & DasSarma, 2017). These extremophiles are not only of ecological interest but also present valuable biotechnological potential, such as the production of salt-tolerant enzymes, bioactive compounds, and compatible solutes (Akpolat et al., 2021). Recent advances in next-generation sequencing (NGS) technologies, particularly 16S rRNA gene amplicon sequencing, have significantly enhanced our understanding of microbial diversity in such ecosystems by enabling culture-independent analysis of complex microbial communities (Vavourakis et al., 2016). This has led to the discovery of numerous novelties or uncultured microbial lineages in hypersaline habitats across the globe. In North Africa, Algeria hosts a diverse array of hypersaline systems such as Sebkhaz-Zemoul, Chott Melrhir, and Zahrez lakes that remain underexplored microbiologically. Several culture-based studies have provided important insights into their microbial diversity. For instance, Menasria et al. (2019) investigated culturable halophilic bacteria from Algerian saline habitats, revealing a wealth of strains with antimicrobial and enzymatic activities. Similarly, Amziane et al. (2013) described *Virgibacillus natechei* sp. nov., isolated from sediment of a southwestern Algerian Salt Lake, while Addou et al. (2013) identified *Melghirimyces thermohalophilus* from an Algerian Salt Lake, highlighting endemic microbial diversity.

Archaea, particularly ammonia-oxidizing archaea (AOA), play a key role in biogeochemical nitrogen cycling across diverse environments, including hypersaline and extreme habitats (Park et al., 2010; Kim et al., 2016). Their ecological significance has been widely demonstrated in both soil and marine systems.

Beyond bacteria, archaeal communities are also a key component of hypersaline environments. Quadri et al. (2016) isolated and characterized extremely halophilic archaea from Algerian Saharan salt pans, showing their adaptation and biotechnological potential. Comparable research in Tunisia by Ben Abdallah et al. (2018) demonstrated the abundance and diversity of prokaryotes in Chott El Jerid, an ephemeral hypersaline lake, using high-throughput sequencing and molecular assays.

Despite these contributions, many Algerian hypersaline systems remain unexplored using modern sequencing tools. In this context, the present study investigates the microbial diversity of two hypersaline environments in central Algeria Hadjer El-Melh and Zahrez-Gharbi using Illumina MiSeq-based 16S rRNA gene amplicon sequencing. By combining physicochemical analysis with taxonomic profiling at multiple levels (phylum,

family, genus, and species), this research provides new insights into microbial community composition, site-specific adaptations, and the potential novelty of microbial taxa in Algerian hypersaline lakes.

2. Materials and methods

Two hypersaline sampling sites were selected from geologically and hydrologically distinct environments within the Djelfa region of Algeria figure 1, both subjected to semi-arid to arid climatic conditions (Peel et al., 2007; ONM, n.d.).

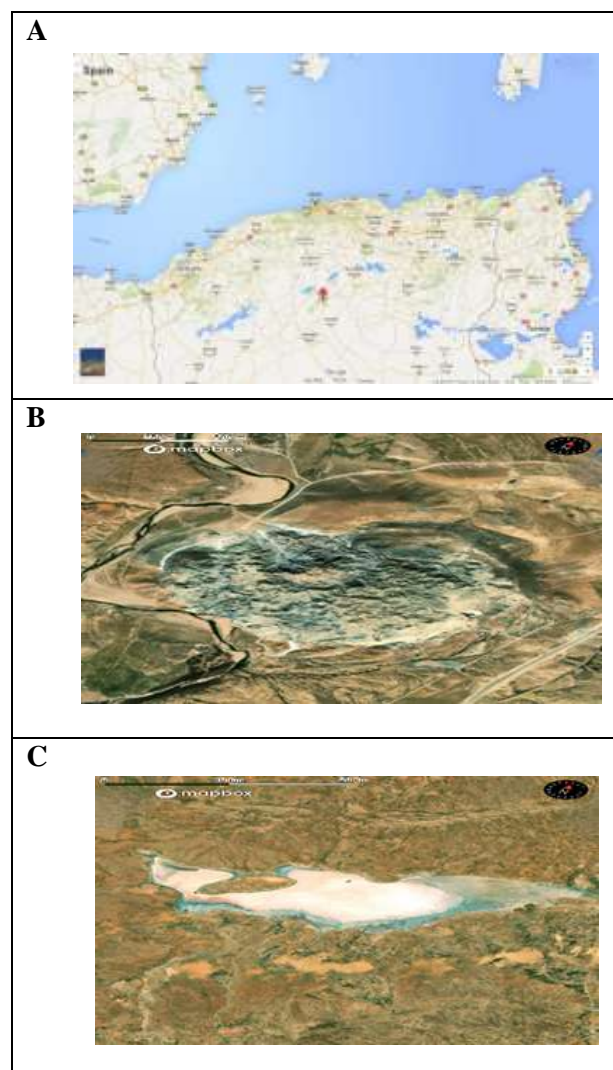


Figure 1. Geographic location of the study area in central Algeria (A), highlighting Hadjer El-Melh (B) and Zahrez-Gharbi (C) regions. (Source Google Earth).

2.1 Sampling sites

Site 1: Hajr El Meleh (Salt Rock) (Latitude: 34.6667° N, Longitude: 3.2500° E). This natural salt outcrop represents an exposed evaporitic deposit, formed through long-term sedimentation and mineral crystallization under arid climatic conditions (Warren, 2010). The site is characterized

by minimal water activity on the surface, with hypersaline brines often confined within salt fissures or shallow depressions. Its high salinity and mineral content make it an extreme environment conducive to the growth of specialized halophilic microorganisms (Oren, 2002). This site experiences a semi-arid continental climate, characterized by hot, dry summers and cold winters. Annual precipitation is low, averaging less than 300 mm, with most rainfall occurring between November and March (ONM, n.d.). Summer temperatures can exceed 38°C, while winter nights may drop below freezing. High evaporation rates and persistent sunlight contribute to the concentration of salts in the area (Warren, 2017).

Site2 : Zahrez-Gharbi Lake (*Latitude : 34.5089° N, Longitude : 2.7184° E*). Is a large endorheic Salt Lake (sebkha) located southwest of Djelfa city. This ephemeral water body exhibits pronounced seasonal variability, with significant changes in water level and salinity driven by high evaporation rates and irregular rainfall (Senni et al., 2020). During the dry season, the lake may partially or completely desiccate, leaving behind salt crusts and concentrated brines (Deocampo & Jones, 2014). The dynamic physicochemical conditions of Zahrez-Gharbi support diverse and adaptable microbial communities, particularly halotolerant and halophilic taxa (Oren, 2002). This region is dominated by an arid to semi-arid climate, with intense summer heat and high evaporation rates exceeding precipitation (Peel et al., 2007; ONM, n.d.). Annual rainfall is sparse, typically under 250 mm, and unevenly distributed. Temperatures in summer regularly reach above 40°C, while winter temperatures are milder compared to the higher-altitude Hadjer El-Melh. Wind activity is frequent, contributing to dust transport and further influencing salinity gradients (Sellam et al., 2019).

2.2. Samples Collection

Two water samples were collected from distinct hypersaline environments located in the Djelfa region, Algeria. The first sample (S1) was taken from the Hadjer El-Melh, and the second sample (S2) was obtained from the saline water of Zahrez-Gharbi Lake, characterized by extensive seasonal fluctuations and high evaporation rates. Both samples were collected on June 10th, 2023.

To assess the physicochemical characteristics of the hypersaline water samples, salinity, pH, and electrical conductivity (EC) were measured immediately after sample collection. Salinity was determined using a handheld refractometer (ATAGO S-28E, Japan), which measures sodium chloride concentration in the range of 0–28%. The

instrument was calibrated before use according to the manufacturer's instructions, and measurements were performed in triplicate for accuracy. Although the S-28E provides NaCl-specific salinity values, it was considered appropriate for the hypersaline nature of the studied environments. pH and electrical conductivity were measured using a portable benchtop multiparameter meter (OHAUS STARTER 300). The device was calibrated using standard buffer solutions (pH 4.0, 7.0, and 10.0) and conductivity standards prior to measurement. Readings were taken on-site to minimize alterations due to storage or temperature shifts. Electrical conductivity (EC) was measured using a portable benchtop conductivity meter (OHAUS STARTER 300C). The instrument was calibrated prior to measurement using certified conductivity standards to ensure accuracy. Measurements were conducted on-site to avoid potential changes in salinity or temperature during sample transport and storage. All measurements were conducted at ambient field temperature, and values were recorded in situ to reflect the original environmental conditions of each sampling site. Samples were collected in sterile, acid-washed polyethylene bottles, transported on ice, and stored at 4 °C until analysis (Lauber et al., 2010; Song et al., 2016; Vass et al., 2020). All sampling procedures were conducted following standard protocols to avoid contamination and ensure sample integrity.

2.3. Physicochemical Analysis

Water samples were filtered through 0.22 µm pore-size membranes prior to analysis to remove suspended particles. The concentrations of major cations (Ca²⁺, Fe, K⁺, Mg²⁺, Mn²⁺, Na⁺) and anions (Cl⁻, NO₃⁻, PO₄³⁻, SO₄²⁻) were measured using inductively coupled plasma–optical emission spectrometry (ICP-OES) and ion chromatography (IC) at a certified laboratory. Detection limits (BG) were defined for each ion based on instrument sensitivity.

2.4. DNA extraction, 16s rRNA Library Preparation and Sequencing

The microbiome total DNA was extracted using the QIAamp DNA Microbiome Kit (Qiagen) according to the manufacturer's protocol. The quality and concentration of the extracted DNA were measured using a NanoDrop spectrophotometer (ND-1000, NanoDrop Technologies, Wilmington, DE, United States). The V3–V4 region of the bacterial 16S-rRNA gene was amplified by PCR (95°C for 5 min, followed by 25 cycles of 95°C for 30 s, 50°C for 30 s, 72°C for 40 s, and 72°C for 7 min) using the

primers 338F (51-ACTCCTACGGGAGGCAGCA-31) and 806R (51-GGACTACHVGGGTWTCTAAT-31) and a high-fidelity polymerase. Indexed adapters were added to the ends of the primers. The PCR products were mixed with the same volume of 2× loading buffer and were subjected to 1.8% agarose gel electrophoresis for detection. Samples with a bright main band of approximately 450 bp were chosen and mixed in equal-density ratios. Then, the mixture of PCR products was purified using a GeneJET Gel Extraction Kit (Thermo Fisher Scientific, Waltham, MA, United States). Sequencing libraries were generated using NEB Next® Ultra™ DNA Library Prep Kit for Illumina (NEB, USA) following manufacturer's recommendations and indexed adapters were added. The constructed libraries were validated using an Agilent 2100 Bioanalyzer (Agilent Technologies, Palo Alto, CA, United States) and quantified with a Qubit 2.0 Fluorometer (Thermo Fisher). Finally, paired-end sequencing was conducted using an Illumina NovaSeq6000 platform (Illumina, Inc., San Diego, CA, United States) with 2x250 bp configuration at CD Genomics, Co., Ltd. (NY, USA). The data underwent several preprocessing steps prior to downstream analysis. Demultiplexing was carried out using unique barcodes assigned to each sample, followed by removal of primer and barcode sequences. Paired-end reads were merged using FLASH v1.2.11 (Magoc & Salzberg, 2011), a tool that accurately combines overlapping paired reads into contiguous sequences (raw tags). Quality filtering of raw tags was performed using Fastp, removing low-quality sequences to yield high-quality clean tags for further analysis.

2.5. Statistical and Bioinformatics Analyses

The raw reads were quality filtered under specific filtering conditions to obtain high-quality clean tags on the basis of the QIIME2 quality control process (Wang et al., 2012; Bolyen et al., 2019). Sequences that were less than 200 bp in length or that contained homopolymers longer than 8 bp were removed. The chimera sequences were detected by comparing tags with the reference database (SILVA) using the UCHIME algorithm (Edgar, 2010) and then removed. The effective sequences were then used in the final analysis. Sequences were grouped into amplicon sequence variant (ASV) using the clustering program DADA2 (version 1.26) (Callahan et al., 2016) against the SILVA bacterial database (Quast et al., 2013) pre-clustered at 97% sequence identity. They were then taxonomically classified to different levels (phylum, class, order, family, genus, and species) using the Ribosomal

Database Program (RDP) classifier. Alpha diversity indices (i.e., ACE, Chao1, Shannon, and Simpson) were calculated by QIIME2 from rarefied samples using for richness and diversity indices of the bacterial community. Beta diversity was calculated using unweighted UniFrac and non-metric multidimensional scaling (NMDS), after which Intra-group and Inter-group beta distance boxplot diagrams were generated. A one-way analysis of similarity (ANOSIM) was performed to determine the differences in bacterial communities among groups (Clarke and Gorley, 2006). Linear discriminant analysis (LDA) effect size (LefSe) analysis was performed to reveal the significant ranking of abundant modules in healthy and diarrheic samples (Segata et al., 2011). A size-effect threshold of 4.0 on the logarithmic LDA score was used for discriminative functional biomarkers. Phylogenetic Investigation of Communities by Reconstruction of Unobserved States (PICRUSt) (Langille et al., 2013) was used to predict the functional gene content in the fecal microbiota based on taxonomy obtained from the Greengenes reference database1 (DeSantis et al., 2006). PICRUSt and LefSe were performed online in the Galaxy workflow framework. Alpha diversity indexes are presented as the means ± SD. The differences in Alpha diversity indexes and top 10 phyla and genera relative abundances between groups were calculated by use of the Independent-sample t-test (for the normally distributed data) or Mann–Whitney U-test (for the non- normally distributed data). A P-value < 0.05 was considered statistically significant, and P-value < 0.01 indicating the differences are extremely significant.

3. Results

3.1. Physicochemical properties

The physicochemical profiles of the two hypersaline water samples Hadjer El-Melh (S1) and Zahrez-Gharbi (S2) are summarized in Table 1. Both sites exhibited extremely high salinity, with S1 reaching 26.5% NaCl and S2 slightly lower at 23.0% NaCl, reflecting the hypersaline nature of the environments. The pH values were near neutral, measured at 6.89 for S1 and 7.02 for S2. Electrical conductivity exceeded the upper measurement range of 200 mS/cm for both samples, confirming the high ionic strength of the waters. Regarding cationic composition, sodium (Na⁺) was the dominant ion, with concentrations of 128,000 mg/L in S1 and 109,000 mg/L in S2. Calcium (Ca²⁺) and magnesium (Mg²⁺) also contributed significantly: Ca²⁺ was higher in S1 (1002.52 mg/L), while Mg²⁺ was markedly elevated in S2 (5450 mg/L). Potassium

(K⁺) concentrations were similar in both samples, ranging between 720 and 764 mg/L. Iron (Fe) and manganese (Mn) were present in low concentrations, with Fe being three times more abundant in S1 (0.124 mg/L) compared to S2 (0.038 mg/L), and Mn showing the reverse trend. Among the anions, chloride (Cl⁻) was predominant, with values of 214,151 mg/L in S1 and 173,571 mg/L in S2. Sulfate (SO₄²⁻) was higher in S2 (15,276 mg/L) than in S1 (5585 mg/L), likely due to underlying lithological or hydrological differences. Nitrate (NO₃⁻) and phosphate (PO₄³⁻) were below the detection threshold in both samples, suggesting minimal influence from agricultural or anthropogenic sources. These data confirm the extreme salinity and ionic complexity of both sites, shaped by evaporitic geology and climatic aridity, and provide a robust basis for interpreting the microbial diversity within these environments.

Table 1. Chemical composition of hypersaline water samples

Parameter (unit)	Hadjer El-Melh(S1)	Zahrez-Gharbi (S2)
pH	6.89	7.02
Salinity (% NaCl)	26.5	23.0
Conductivity (mS/cm)	>200	>200
Ca ²⁺ (mg/L)	1002.52	430.64
Fe (mg/L)	0.124	0.038
K ⁺ (mg/L)	720	764
Mg ²⁺ (mg/L)	322	5450
Mn ²⁺ (mg/L)	0.856	0.026
Na ⁺ (mg/L)	128000	109000
Chloride Cl ⁻ (mg/L)	214151	173571
Nitrate NO ₃ ⁻ (mg/L)	< BG	< BG
Phosphate PO ₄ ³⁻ (mg/L)	< BG	< BG
Sulfate SO ₄ ²⁻ (mg/L)	5585	15276

*BG: < limite de détection.

3.2. Sequencing Quality Statistics

The Illumina sequencing generated a total of 471134 and approximately 437000 raw reads for samples S01 and S02, respectively (Table 2). After quality filtering and chimera removal, 173190 and 141532 high-quality clean reads were retained. The average read lengths were 414 bp for S01 and 378 bp for S02. The GC content ranged from 53.33% to 54.95%, indicating relatively stable nucleotide composition across samples. Quality assessment showed high sequencing accuracy, with Q20 values exceeding 97% and Q30 values above 92% for both samples, confirming the reliability of the sequencing data for downstream analyses Table 2. To visualize the read distribution, a histogram was generated showing the

length distribution of merged reads. Figure 2 illustrates the number of sequences

Table 2. Summary statistics of raw reads and quality-controlled tags for samples S01 and S02.

Parameter	S01	S02
Raw Reads (nt)	471134	437000
Clean Tags (nt)	173190	141532
Avg Length (nt)	414	378
GC Content (%)	53.33	54.95
Q20 (%)	97.83	98.37
Q30 (%)	92.9	94.16

nt: nucleotides.

PE Reads: Paired-end reads from the sequencing platform. Clean Tags: Reads retained after quality control. Q20 and Q30: Percentage of bases with Phred quality scores ≥20 and ≥30, respectively.

plotted against sequence length for sample S01. A dominant peak around 440–460 nt was observed, consistent with the expected amplicon length. Additional graphs for other samples are available in the supplementary results

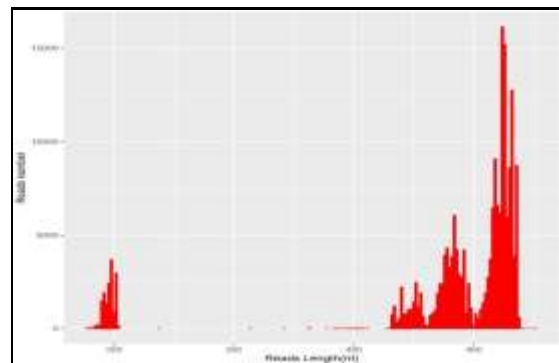


Figure 2. Length distribution of merged 16S rRNA reads the histogram shows the number of reads across different sequence lengths after quality filtering and merging. A prominent peak is observed around 440–460 bp, indicating successful amplification of the target region.

After quality filtering and denoising with DADA2 in QIIME 2 (Hall & Beiko, 2018), a total of 60,000 high-quality sequence reads were retained across both samples. Sample S01 contributed approximately 26,000 reads, while Sample S02 (Zahrez-Gharbi) yielded around 34,000 reads (Figure 3A). Amplicon sequence variants (ASVs) were then identified based on 100% sequence identity. The resulting feature table revealed that most ASVs were of low to moderate abundance, while a smaller number were highly dominant across the dataset (Figure 3B). These ASVs served as the

basis for downstream taxonomic and diversity analyses, offering a high-resolution representation of microbial community structure.

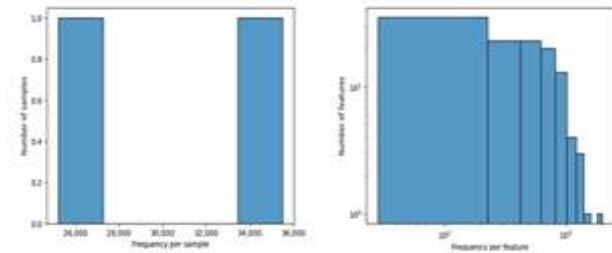


Figure 3. (A) Left: Histogram showing sequencing depth per sample. Sample S01 (Hadjer El-Melh) yielded approximately 26,000 reads, and Sample S02 (Zahrez-Gharbi) yielded approximately 34,000 reads. (B) Right: Histogram showing the distribution of ASV abundance (frequency per feature). Most ASVs occurred at low frequencies, while a small number of dominant ASVs had high read counts, reflecting the typical rank-abundance pattern in microbial communities.

3.3. Microbial Community Structure and Diversity

The bar plot shown in the Figure 4 illustrates the relative abundance of dominant microbial phyla in two hypersaline water samples. Both samples are dominated by Firmicutes, Bacteroidota, and Proteobacteria, with Actinobacteriota and Halanaerobiota also contributing significantly. Notably, archaeal phyla such as Halobacterota, Euryarchaeota, and Nanoarchaeota are present in lower proportions, reflecting archaeal adaptation to high-salt conditions. A histogram displaying the taxonomic distribution at the phylum level is shown

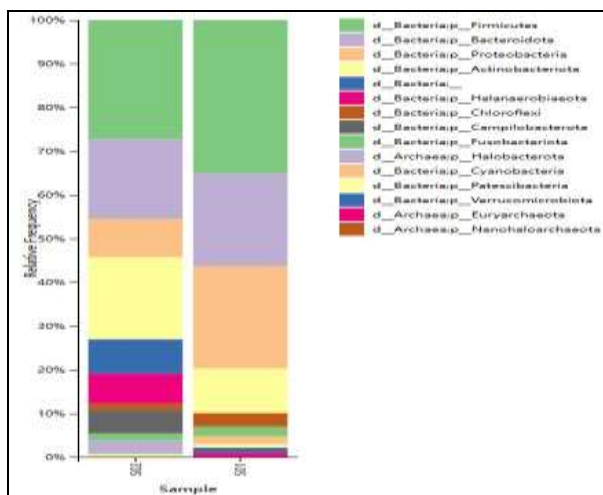


Figure 4. The taxonomy bar plot distribution of all sample in Phylum classification level. Additional taxonomic classifications are available in the data submitted to NCBI and Zenodo repositories.

in Figure 5. Each color in the chart represents a distinct phylum, with the length of the bars

indicating their relative abundance in the microbial community. For clarity and readability, only the top 10 most abundant phyla are displayed; phyla with lower abundance have been grouped under the label “Others.” Taxa that could not be annotated are marked as “Unknown.” Based on the taxonomic composition and relative abundance of microbial communities in each sample, heatmap analyses were performed across multiple taxonomic ranks (phylum, class, order, family, genus, and species). These heatmaps were generated using R language tools to visualize abundance patterns and similarity relationships. In the heatmap (Figure 4), color intensity represents the relative abundance of each taxon, with darker shades indicating higher abundance. Vertical clustering reflects the similarity of taxa based on their distribution patterns across samples, where shorter branch lengths indicate more closely related abundance profiles. Horizontal clustering reflects the similarity of microbial community composition between samples, with shorter distances implying greater similarity. The heatmap at the phylum level is shown in Figure 5, highlighting dominant microbial groups and allowing a comparative view of taxonomic distribution across the two hypersaline environments. Alpha diversity represents the within-sample microbial diversity, measuring species richness and evenness. In this study, four commonly used indices were calculated:

- Chao1 and ACE: Estimators of species richness (the number of unique taxa).
- Shannon and Simpson: Indices that account for both richness and evenness of the microbial community.

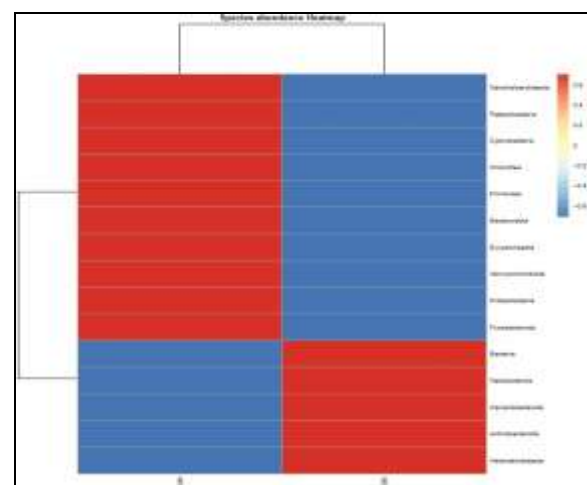


Figure 5. Species abundance Heatmap. Phylum. Plotted by sample name on the X-axis. The Y-axis represents the genus. The absolute value of the legend represents the distance between the raw score and the mean population of the standard deviation. The legend is negative when the raw score is below the mean.

Higher values of Chao1, ACE, and Shannon indices indicate greater microbial diversity (Grice et al., 2009), while lower Simpson index values also reflect higher community complexity. Additionally, library coverage was used to assess sequencing completeness; a higher value suggests a higher probability that a given sequence present in the environment is captured by the sequencing process, reflecting the representativeness of the microbial population.

To ensure a fair comparison, sequence counts were normalized across samples during analysis. Alpha diversity metrics were calculated at a 97% similarity threshold and are presented in Table 3. Sample S1 (Hadjer El-Melh) exhibited greater microbial diversity than Sample S2 (Zahrez-Gharbi), as indicated by higher values of the Chao1, ACE, and Shannon indices. This suggests a richer and more evenly distributed microbial community in this environment.

Table 3. Statistics of Alpha diversity indices.

Parameter	S1	S2
Observed Species	73	50
ACE	73	50
Chao1	73	50
Simpson	0.98	0.967
Shannon	5.827	5.225

Rarefaction analysis was performed to assess the sequencing depth and microbial richness of the samples. The rarefaction curve was generated by randomly subsampling the sequencing reads and plotting the number of observed species (Shannon diversity index) against sequencing depth.

As shown in Figure 6 (top), the curve exhibits a steep rise at lower sequencing depths, indicating that additional sequencing initially uncovers a large number of new taxa. However, as the sequencing depth increases, the curve gradually flattens, demonstrating that most of the microbial diversity has been captured and additional sequencing would yield diminishing returns in terms of novel taxa detection. This plateau confirms that the sequencing depth was sufficient for both samples to provide reliable estimates of microbial diversity. Figure 6 (bottom) shows the number of samples analyzed at each sequencing depth, confirming consistent sampling across the dataset. The taxonomic profiling at the phylum level revealed notable differences in microbial community structure between the two hypersaline samples (S01 – Hadjer El-Melh, and S02 – Zahrez-Gharbi) Figure 7. In both samples, the dominant phyla belonged to the domain Bacteria. Firmicutes

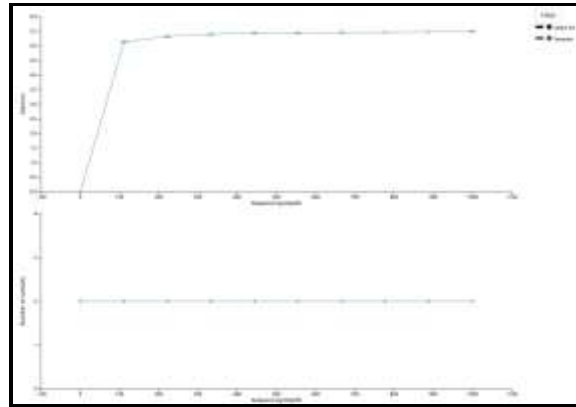


Figure 6. Top: Rarefaction curve based on the Shannon diversity index showing the relationship between sequencing depth and species richness for both samples. Bottom: Sample count across sequencing depths, confirming even sampling coverage.

was the most abundant phylum in both samples, particularly in S01 (12,469 reads) compared to S02 (6,864 reads). Similarly, Proteobacteria and Bacteroidota were highly represented in both environments, although with different relative abundances: Proteobacteria (8,288 in S01 vs. 2,199 in S02) and Bacteroidota (7,524 in S01 vs. 4,612 in S02). Other bacterial phyla such as Actinobacteriota, Chloroflexi, and Fusobacteriota were also present in both samples, with Actinobacteriota slightly more abundant in S02 (4,750) than in S01 (3,640), and Chloroflexi showing a higher presence in S01 (1,111) than in S02 (378). Notably, Halanaerobiaeota, Campilobacterota, and unknown bacteria were detected exclusively in S02, while Verrucomicrobiota, Cyanobacteria, and Patescibacteria were only found in S01. In terms of archaeal diversity, Euryarchaeota and Nanohaloarchaeota were exclusively detected in S01, whereas Halobacterota was only observed in S02 (773 reads). These findings highlight site-specific microbial diversity and the potential influence of environmental and physicochemical conditions on community composition in hypersaline ecosystems.

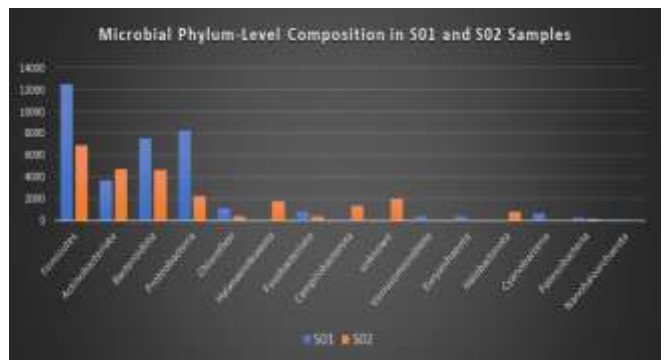


Figure 7. Abundance of microbial phyla identified in hypersaline samples S01 (Hadjer El-Melh) and S02 (Zahrez-Gharbi).

Microbial community analysis at the family level revealed clear differences in taxonomic profiles between the two hypersaline sites. A total of over 40 bacterial and archaeal families were detected across both samples, with several taxa exhibiting site-specific distribution patterns Figure 8. In both samples, Staphylococcaceae, Corynebacteriaceae, Prevotellaceae, and Rhodothermaceae were among the most dominant families. Notably, Corynebacteriaceae was more abundant in S02 (3,331 reads) than in S01 (1,366 reads), while Rhodothermaceae showed higher abundance in S01 (2,484) than in S02 (866). Some families, such as Clostridia_UCG.014, Gitt.GS.136, Moraxellaceae, Halomonadaceae, and Lactobacillaceae, were exclusively detected in S01, suggesting a strong influence of the Hadjer El-Melh environment on microbial selection. Conversely, S02 was characterized by the exclusive presence of several families, including Balneolaceae (1,013 reads), Bacillaceae (1,218), Veillonellaceae (995), Halobacteroidaceae (1,719), and Micrococcaceae (1,256). Additionally, Campylobacteraceae and archaeal Haloferacaceae were found only in S02, while Methanobacteriaceae and Nanosalinaceae were detected only in S01. The occurrence of unclassified families such as "Unknown Bacteria", "Unknown Proteobacteria", and "Unknown Alphaproteobacteria" further indicates the presence of uncultured or poorly characterized microbial taxa in these extreme hypersaline environments.

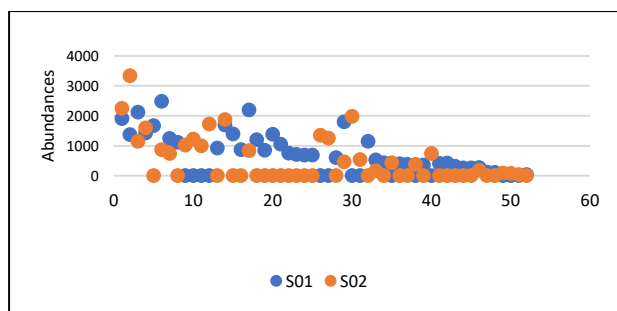


Figure 8. Abundance of microbial families in hypersaline samples S01 (Hadjer El-Melh) and S02 (Zahrez-Gharbi). Shared families include Staphylococcaceae, Corynebacteriaceae, and Rhodothermaceae, while several taxa exhibit site-specific patterns. Archaeal families and unclassified groups highlight the distinct and complex microbial communities shaped by each environment.

A genus-level comparative analysis figure 9 revealed significant variations in microbial community composition between the two hypersaline samples (S01: Hadjer El-Melh and S02: Zahrez-Gharbi). Among the top 20 most abundant genera, *Corynebacterium*, *Staphylococcus*, *Porphyromonas*, and *Alloprevotella* were commonly

abundant in both samples. However, notable differences were observed: *Salinibacter*, *Clostridia_UCG.014*, and *Finegoldia* were dominant in S01 but absent in S02, while *Campylobacter*, *Bacillus*, and *Veillonella* were specifically enriched in S02. These genera-level shifts highlight the ecological uniqueness of each hypersaline environment and reflect adaptation to localized physicochemical conditions

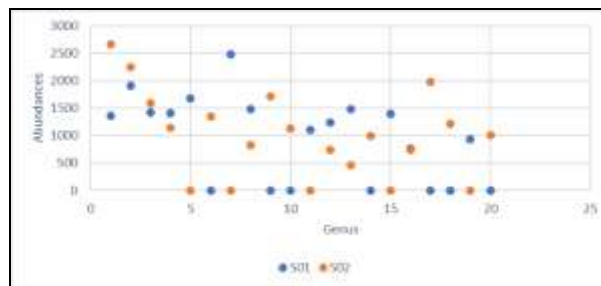


Figure 9. Relative abundances of the top 20 most dominant microbial genera in hypersaline samples S01 (blue) and S02 (orange). Each point corresponds to the abundance of a specific genus. Shared genera such as *Staphylococcus* and *Corynebacterium* are prominent in both samples, while others exhibit sample-specific patterns, reflecting site-dependent microbial composition.

At the species level (Figure 10), the microbial communities of samples S01 and S02 displayed both overlapping and sample-specific taxa. A total of 35 distinct species were identified, with 21 species exclusive to S01, 9 unique to S02, and only 5 species shared between both sites. *Staphylococcus carnosus* was the most dominant species in both samples, showing higher abundance in S02 (2245 reads) compared to S01 (1908 reads). Similarly, *Porphyromonas* and *Corynebacterium* (unclassified at the species level) were present in both samples but exhibited greater abundance in S02. In contrast, S01 harbored several exclusive and highly abundant species, including *Salinibacter* (2484), *Finegoldia magna* (929), and *Clostridia_UCG.014* (uncultured *Lactococcus*) (1672), all absent from S02. Zahrez-Gharbi (S02), on the other hand, contained site-specific taxa such as *Bacillus* (1218), *Campylobacter* (unidentified; 1345), *Veillonella* (995), and *Orenia* (1719), which were completely absent in S01. Several unidentified or uncultured taxa were detected in both samples, including *Corynebacterium*, *Comamonadaceae*, and *Halomonadaceae*, indicating the presence of potentially novel or uncharacterized microbial lineages. These findings reflect strong environmental filtering and highlight site-specific microbial adaptation to the physicochemical characteristics of each hypersaline habitat.

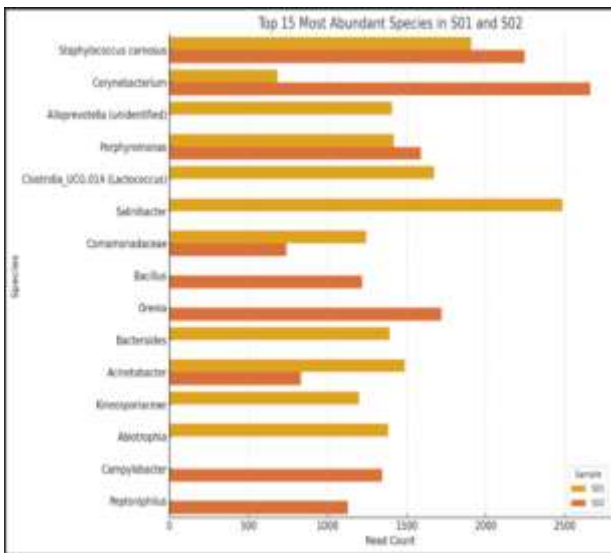


Fig. 10. Bar chart showing the abundance of the 15 most dominant microbial species detected in hypersaline samples S01 (orange) and S02 (dark orange).

While *Staphylococcus carnosus* and *Corynebacterium* were highly abundant in both samples, most species exhibited strong site-specific patterns. *Salinibacter*, *Clostridia_UCG.014* (uncultured *Lactococcus*), and *Allopevotella* were dominant in S01, whereas *Orenia*, *Bacillus*, and *Campylobacter* were uniquely abundant in S02. This distribution highlights the influence of environmental selection and microbial niche specialization within these saline ecosystems.

4. Discussion:

The extreme salinities observed (26.5% and 23.0% NaCl) and high ionic strengths in both Hadjer El-Melh (S1) and Zahrez-Gharbi (S2) are typical of saturated brines, conditions known to favor highly specialized halophiles and limit overall diversity (Ventosa et al., 1998, 2015). The dominance of Na⁺ and Cl⁻, along with comparative differences in Mg²⁺ and SO₄²⁻ concentrations, likely shapes the specific microbial communities found at each site (Oren, 2010). Our taxonomic profiling across hierarchical levels—phylum to species—revealed substantial shifts between the two samples. Notably, *Salinibacter* (Bacteroidetes) was highly abundant in S1 but absent from S2. This aligns with its known ecology as a model extreme halophile that thrives in ≥20% salt environments alongside haloarchaea (Antón et al., 2002; Ventosa et al., 2015). Similarly, the detection of *Methanobrevibacter smithii* and other archaeal taxa in S1 reflects archaeal adaptation to high salinity conditions (García-Maldonado et al., 2023). The presence of Halobacterota in S2 further supports the role of lithology and salinity gradients in determining archaeal community composition.

The presence of ammonia-oxidizing archaea (AOA), particularly within the Halobacterota phylum detected in S2, may indicate nitrification potential in hypersaline conditions, despite extreme osmotic stress. This observation aligns with the work of Rhee and colleagues, who successfully enriched AOA from marine and estuarine sediments and demonstrated their ecological versatility under various salinity and oxygen conditions (Park et al., 2010). In particular, their studies on hydrogen peroxide detoxification mechanisms in Thaumarchaeota highlight the biochemical adaptations that allow these archaea to persist in oxidative environments (Kim et al., 2016). Such resilience may explain the dominance of Halobacterota in Zahrez-Gharbi, where fluctuating ionic and oxidative conditions prevail. These insights support the hypothesis that archaeal communities in hypersaline ecosystems are not only taxonomically diverse but also functionally specialized to cope with harsh geochemical regimes. Alpha diversity indices (Chao1, ACE, Shannon) and rarefaction analyses demonstrated greater microbial richness and evenness in S1 relative to S2. This pattern is consistent with diversity trends in hypersaline habitats, where moderate salinities (around 20–30%) support maximum taxonomic richness, while higher salinities suppress it (Ovreås et al., 2003). Distinct clustering patterns in heatmaps and classification trees underscore marked differences in community structure between the two sites. Genera such as *Clostridia_UCG.014*, *Salinibacter*, and *Acinetobacter* were specific to S1, suggesting specialized adaptation to halite rock-hosted niches. In contrast, *Campylobacter*, *Bacillus*, *Orenia*, and *Halobacteraceae* appeared only in S2, indicating adaptation to sediment or brine-lake conditions with different geochemical dynamics. The species-level microbial profiles of S01 (Hadjer El-Melh) and S02 (Zahrez-Gharbi) reflect strong ecological differentiation shaped by site-specific physicochemical conditions. While shared taxa such as *Staphylococcus carnosus* and *Porphyromonas* were abundant in both environments, most other species exhibited distinct site preferences. S01, for example, was dominated by *Salinibacter*, *Finegoldia magna*, and an uncultured *Lactococcus* (*Clostridia_UCG.014*), which are typical of highly saline, possibly anaerobic niches. In contrast, S02 harbored unique taxa such as *Orenia*, *Campylobacter*, *Bacillus*, and *Veillonella*, suggesting a different set of environmental pressures or available niches. The detection of multiple unclassified or uncultured lineages such as unidentified *Corynebacterium*, *Comamonadaceae*, and *Halomonadaceae* further underscores the

novelty and complexity of microbial life in these hypersaline systems. These site-specific community structures are consistent with previous studies in extreme environments, where salinity, oxygen availability, and nutrient gradients are key drivers of microbial diversity and specialization (Ventosa et al., 2015; Telesh et al., 2013). Our findings emphasize the importance of integrating geochemical profiling with high-resolution sequencing to understand microbial ecology in extreme environments. The presence of uncultured and novel taxa-like unknown Comamonadaceae and Halomonadaceae highlights the untapped microbial diversity in hypersaline systems. Future work using metagenomics or targeted cultivation may help uncover novel adaptive pathways and metabolic capabilities, especially among dominant archaeal lineages like *Methanobrevibacter* and *Halobacterota*. Beyond microbial diversity alone, these findings hold important implications for environmental management. Understanding microbial diversity in hypersaline ecosystems is essential not only for advancing microbial ecology but also for informing sustainable environmental management strategies. Microorganisms in such extreme habitats contribute to key biogeochemical processes, including nitrogen and sulfur cycling, which influence water quality and mineral precipitation (Oren, 2010; Kim et al., 2016). Moreover, profiling microbial communities can serve as a bioindicator approach for monitoring salinity fluctuations and anthropogenic impacts in fragile Salt Lake and Salt Rock systems (Ventosa et al., 2015; Park et al., 2010). Integrating microbial datasets with geochemical parameters enables data-driven decision-making in the conservation and restoration of saline ecosystems, especially in arid regions like central Algeria.

5. Conclusion

This study highlights the distinct microbial diversity of two hypersaline environments in central Algeria, Hadjer El-Melh and Zahrez-Gharbi, shaped by extreme salinity and ionic composition. Despite harsh conditions, both sites harbored diverse and specialized microbial communities with clear taxonomic and ecological differences. Hadjer El-Melh exhibited higher richness and evenness, while Zahrez-Gharbi showed a distinct community adapted to brine-lake conditions. The presence of numerous unclassified taxa in both environments underscores the significant potential for discovering novel microbial lineages. Overall, these findings demonstrate that salinity, geochemistry, and habitat type are

key drivers of microbial community structure in hypersaline ecosystems. Future studies using advanced omics approaches are needed to further explore the functional roles and biotechnological potential of these extremophiles.

Data availability statement:

All raw sequencing data have been deposited in the NCBI Sequence Read Archive under BioProject **PRJNA1290669**, including BioSamples **SAMN49931787** (Zahrez-Gharbi, S2) and **SAMN49931788** (Hadjer El-Melh, S1), and SRA accessions **SRR34506019** and **SRR34506018**.

Author Statements:

- **Ethical approval:** The conducted research is not related to either human or animal use.
- **Conflict of interest:** The authors declare that they have no known competing financial interests or personal relationships that could have appeared to influence the work reported in this paper
- **Acknowledgement:** The authors declare that they have nobody or no-company to acknowledge.
- **Author contributions:** The authors declare that they have equal right on this paper.
- **Funding information:** The authors declare that there is no funding to be acknowledged.

References

1. Oren, A. (2010). Thermodynamic limits to microbial life at high salt concentrations. *Environmental Microbiology*, 13(8), 1908–1923. Portico. <https://doi.org/10.1111/j.1462-2920.2010.02365.x>
2. Ventosa, A., de la Haba, R. R., Sánchez-Porro, C., & Papke, R. T. (2015). Microbial diversity of hypersaline environments: a metagenomic approach. *Current Opinion in Microbiology*, 25, 80–87. <https://doi.org/10.1016/j.mib.2015.05.002>
3. DasSarma, S., & DasSarma, P. (2015). Halophiles and their enzymes: negativity put to good use. *Current Opinion in Microbiology*, 25, 120–126. <https://doi.org/10.1016/j.mib.2015.05.009>
4. Akpolat, C., Fernández, A. B., Caglayan, P., Calli, B., Birbir, M., & Ventosa, A. (2021). Prokaryotic Communities in the Thalassohaline Tuz Lake, Deep Zone, and Kayacik, Kaldirim and Yavsan Salterns (Turkey) Assessed by 16S rRNA Amplicon Sequencing. *Microorganisms*, 9(7), 1525. <https://doi.org/10.3390/microorganisms9071525>

5. Vavourakis, C. D., Ghai, R., Rodriguez-Valera, F., Sorokin, D. Y., Tringe, S. G., Hugenholtz, P., & Muyzer, G. (2016). Metagenomic Insights into the Uncultured Diversity and Physiology of Microbes in Four Hypersaline Soda Lake Brines. *Frontiers in Microbiology*, 7. <https://doi.org/10.3389/fmicb.2016.00211>
6. Menasria, T., Monteoliva-Sánchez, M., Benammar, L., Benhadj, M., Ayachi, A., Hacène, H., Gonzalez-Paredes, A., & Aguilera, M. (2019). Culturabile halophilic bacteria inhabiting Algerian saline ecosystems: A source of promising features and potentialities. *World Journal of Microbiology and Biotechnology*, 35(9). <https://doi.org/10.1007/s11274-019-2705-y>
7. Amziane, M., Metiaz, F., Darenfed-Bouanane, A., Djenane, Z., Selama, O., Abderrahmani, A., Cayol, J.-L., & Fardeau, M.-L. (2013). *Virgibacillus natechei* sp. nov., A Moderately Halophilic Bacterium Isolated from Sediment of a Saline Lake in Southwest of Algeria. *Current Microbiology*, 66(5), 462–466. <https://doi.org/10.1007/s00284-012-0300-7>
8. Addou, A. N., Schumann, P., Spröer, C., Bouanane-Darenfed, A., Amarouche-Yala, S., Hacene, H., Cayol, J.-L., & Fardeau, M.-L. (2013). *Melghirimycesthermohalophilus* sp. nov., a thermoactinomycete isolated from an Algerian salt lake. *International Journal of Systematic and Evolutionary Microbiology*, 63(Pt_5), 1717–1722. <https://doi.org/10.1099/ijs.0.043760-0>
9. Park, B.-J., Park, S.-J., Yoon, D.-N., Schouten, S., Sinninghe-Damsté, J. S., & Rhee, S.-K. (2010). Cultivation of Autotrophic Ammonia-Oxidizing Archaea from Marine Sediments in Coculture with Sulfur-Oxidizing Bacteria. *Applied and Environmental Microbiology*, 76(22), 7575–7587. <https://doi.org/10.1128/aem.01478-10>
10. Kim, J.-G., Park, S.-J., Sinninghe-Damsté, J. S., Schouten, S., Rijpstra, W. I. C., Jung, M.-Y., Kim, S.-J., Gwak, J.-H., Hong, H., Si, O.-J., Lee, S., Madsen, E. L., & Rhee, S.-K. (2016). Hydrogen peroxide detoxification is a key mechanism for growth of ammonia-oxidizing archaea. *Proceedings of the National Academy of Sciences*, 113(28), 7888–7893. <https://doi.org/10.1073/pnas.1605501113>
11. Quadri, I., Hassani, I. I., l'Haridon, S., Chalopin, M., Hacène, H., & Jebbar, M. (2016). Characterization and antimicrobial potential of extremely halophilic archaea isolated from hypersaline environments of the Algerian Sahara. *Microbiological Research*, 186–187, 119–131. <https://doi.org/10.1016/j.micres.2016.04.003>
12. Ben Abdallah, M., Karray, F., Kallel, N., Armougom, F., Mhiri, N., Quéméneur, M., Cayol, J.-L., Erauso, G., & Sayadi, S. (2018). Abundance and diversity of prokaryotes in ephemeral hypersaline lake Chott El Jerid using Illumina Miseq sequencing, DGGE and qPCR assays. *Extremophiles*, 22(5), 811–823. <https://doi.org/10.1007/s00792-018-1040-9>
13. Peel, M. C., Finlayson, B. L., & McMahon, T. A. (2007). Updated world map of the Köppen-Geiger climate classification. *Hydrology and earth system sciences*, 11(5), 1633–1644.
14. Office National de la Météorologie (ONM). (n.d.). *Climat de la région de Djelfa*. Algeria. [Internal Meteorological Report]
15. Warren, J. K. (2010). Evaporites through time: Tectonic, climatic and eustatic controls in marine and nonmarine deposits. *Earth-Science Reviews*, 98(3–4), 217–268. <https://doi.org/10.1016/j.earscirev.2009.11.004>
16. Oren A. (2002). Molecular ecology of extremely halophilic Archaea and Bacteria. *FEMS microbiology ecology*, 39(1), 1–7. <https://doi.org/10.1111/j.1574-6941.2002.tb00900.x>
17. Warren, J. K. (2017). Salt usually seals, but sometimes leaks: Implications for mine and cavern stabilities in the short and long term. *Earth-Science Reviews*, 165, 302–341. <https://doi.org/10.1016/j.earscirev.2016.11.008>
18. Rachida, S., Gerard, D. B., & Hacene, A. (2020). BIODIVERSITY OF HALOPHYTES IN SEMI-ARID REGIONS CASE OF ZAHREZ GHARBI AND ZAHREZ CHERGUI (ZAAFRANE-DJELFA) IN ALGERIA. *PONTE International Scientific Researches Journal*, 76(11). <https://doi.org/10.21506/j.ponte.2020.11.13>
19. Deocampo, D. M., & Jones, B. F. (2014). *Geochemistry of Saline Lakes*. Treatise on Geochemistry, 437–469. <https://doi.org/10.1016/b978-0-08-095975-7.00515-5>
20. Sellam, N., Viñolas, A., Zougaghe, F., & Moulai, R. (2019). Assessment of the physico-chemical and biological quality of surface waters in arid and semi-arid regions of Algeria (North-Africa). *Bull. Soc. zool. Fr*, 144, 157–178.
21. Lauber, C. L., Zhou, N., Gordon, J. I., Knight, R., & Fierer, N. (2010). Effect of storage conditions on the assessment of bacterial community structure in soil and human-associated samples. *FEMS Microbiology Letters*, 307(1), 80–86. <https://doi.org/10.1111/j.1574-6968.2010.01965.x>
22. Song, S. J., Amir, A., Metcalf, J. L., Amato, K. R., Xu, Z. Z., Humphrey, G., & Knight, R. (2016). Preservation Methods Differ in Fecal Microbiome Stability, Affecting Suitability for Field Studies. *MSystems*, 1(3). <https://doi.org/10.1128/msystems.00021-16>
23. Vass, M., Székely, A. J., Lindström, E. S., & Langenheder, S. (2020). Using null models to compare bacterial and microeukaryotic metacommunity assembly under shifting environmental conditions. *Scientific Reports*, 10(1). <https://doi.org/10.1038/s41598-020-59182-1>
24. Magoč, T., & Salzberg, S. L. (2011). FLASH: fast length adjustment of short reads to improve genome assemblies. *Bioinformatics*, 27(21), 2957–2963. <https://doi.org/10.1093/bioinformatics/btr507>
25. Wang, Y., Sheng, H.-F., He, Y., Wu, J.-Y., Jiang, Y.-X., Tam, N. F.-Y., & Zhou, H.-W. (2012).

- Comparison of the Levels of Bacterial Diversity in Freshwater, Intertidal Wetland, and Marine Sediments by Using Millions of Illumina Tags. *Applied and Environmental Microbiology*, 78(23), 8264–8271. <https://doi.org/10.1128/aem.01821-12>
26. Bolyen, E., Rideout, J.R., Dillon, M.R. et al. Reproducible, interactive, scalable and extensible microbiome data science using QIIME 2. *Nat Biotechnol* 37, 852–857 (2019). <https://doi.org/10.1038/s41587-019-0209-9>
 27. Edgar, R. C. (2010). Search and clustering orders of magnitude faster than BLAST. *Bioinformatics*, 26(19), 2460–2461. <https://doi.org/10.1093/bioinformatics/btq461>
 28. Callahan, B. J., McMurdie, P. J., Rosen, M. J., Han, A. W., Johnson, A. J. A., & Holmes, S. P. (2016). DADA2: High-resolution sample inference from Illumina amplicon data. *Nature Methods*, 13(7), 581–583. <https://doi.org/10.1038/nmeth.3869>
 29. Quast, C., Pruesse, E., Yilmaz, P., Gerken, J., Schweer, T., Yarza, P., Peplies, J., & Glöckner, F. O. (2012). The SILVA ribosomal RNA gene database project: improved data processing and web-based tools. *Nucleic Acids Research*, 41(D1), D590–D596. <https://doi.org/10.1093/nar/gks1219>
 30. Clarke, K. R., and Gorley, R. N. (2006). *Primer v6: User Manual/Tutorial*. Plymouth: Plymouth Marine Laboratory.
 31. Segata, N., Izard, J., Waldron, L., Gevers, D., Miropolsky, L., Garrett, W. S., & Huttenhower, C. (2011). Metagenomic biomarker discovery and explanation. *Genome Biology*, 12(6). <https://doi.org/10.1186/gb-2011-12-6-r60>
 32. Langille, M. G. I., Zaneveld, J., Caporaso, J. G., McDonald, D., Knights, D., Reyes, J. A., Clemente, J. C., Burkipple, D. E., Vega Thurber, R. L., Knight, R., Beiko, R. G., & Huttenhower, C. (2013). Predictive functional profiling of microbial communities using 16S rRNA marker gene sequences. *Nature Biotechnology*, 31(9), 814–821. <https://doi.org/10.1038/nbt.2676>
 33. DeSantis, T. Z., Hugenholtz, P., Larsen, N., Rojas, M., Brodie, E. L., Keller, K., Huber, T., Dalevi, D., Hu, P., & Andersen, G. L. (2006). Greengenes, a Chimera-Checked 16S rRNA Gene Database and Workbench Compatible with ARB. *Applied and Environmental Microbiology*, 72(7), 5069–5072. <https://doi.org/10.1128/aem.03006-05>
 34. Hall, M., & Beiko, R. G. (2018). 16S rRNA Gene Analysis with QIIME2. *Microbiome Analysis*, 113–129. https://doi.org/10.1007/978-1-4939-8728-3_8
 35. Grice, E. A., Kong, H. H., Conlan, S., Deming, C. B., Davis, J., Young, A. C., Bouffard, G. G., Blakesley, R. W., Murray, P. R., Green, E. D., Turner, M. L., & Segre, J. A. (2009). Topographical and Temporal Diversity of the Human Skin Microbiome. *Science*, 324(5931), 1190–1192. <https://doi.org/10.1126/science.1171700>
 36. Ventosa, A., Nieto, J. J., & Oren, A. (1998). Biology of Moderately Halophilic Aerobic Bacteria. *Microbiology and Molecular Biology Reviews*, 62(2), 504–544. <https://doi.org/10.1128/membr.62.2.504-544.1998>
 37. Antón, J., Oren, A., Benlloch, S., Rodríguez-Valera, F., Amann, R., & Rosselló-Mora, R. (2002). *Salinibacterruber* gen. nov., sp. nov., a novel, extremely halophilic member of the Bacteria from saltern crystallizer ponds. *International Journal of Systematic and Evolutionary Microbiology*, 52(2), 485–491. <https://doi.org/10.1099/00207713-52-2-485>
 38. García-Maldonado, J. Q., Latisnere-Barragán, H., Escobar-Zepeda, A., Cadena, S., Ramírez-Arenas, P. J., Vázquez-Juárez, R., Maurilia, R.-C., & López-Cortés, A. (2022). Revisiting microbial diversity in hypersaline microbial mats from Guerrero Negro for a better understanding of methanogenic archaeal communities. <https://doi.org/10.21203/rs.3.rs-2281927/v1>
 39. Ovreås, L., Forney, L., Daae, F. L., & Torsvik, V. (1997). Distribution of bacterioplankton in meromictic Lake Saelenvannet, as determined by denaturing gradient gel electrophoresis of PCR-amplified gene fragments coding for 16S rRNA. *Applied and Environmental Microbiology*, 63(9), 3367–3373. <https://doi.org/10.1128/aem.63.9.3367-3373.1997>
 40. Telesh, I., Schubert, H., & Skarlato, S. (2013). Life in the salinity gradient: Discovering mechanisms behind a new biodiversity pattern. *Estuarine, Coastal and Shelf Science*, 135, 317–327. <https://doi.org/10.1016/j.ecss.2013.10.013>